Wang et al. State-dependent central synaptic regulation by GLP-1 is essential for energy homeostasis

Extended Data Figures and Figure Legends

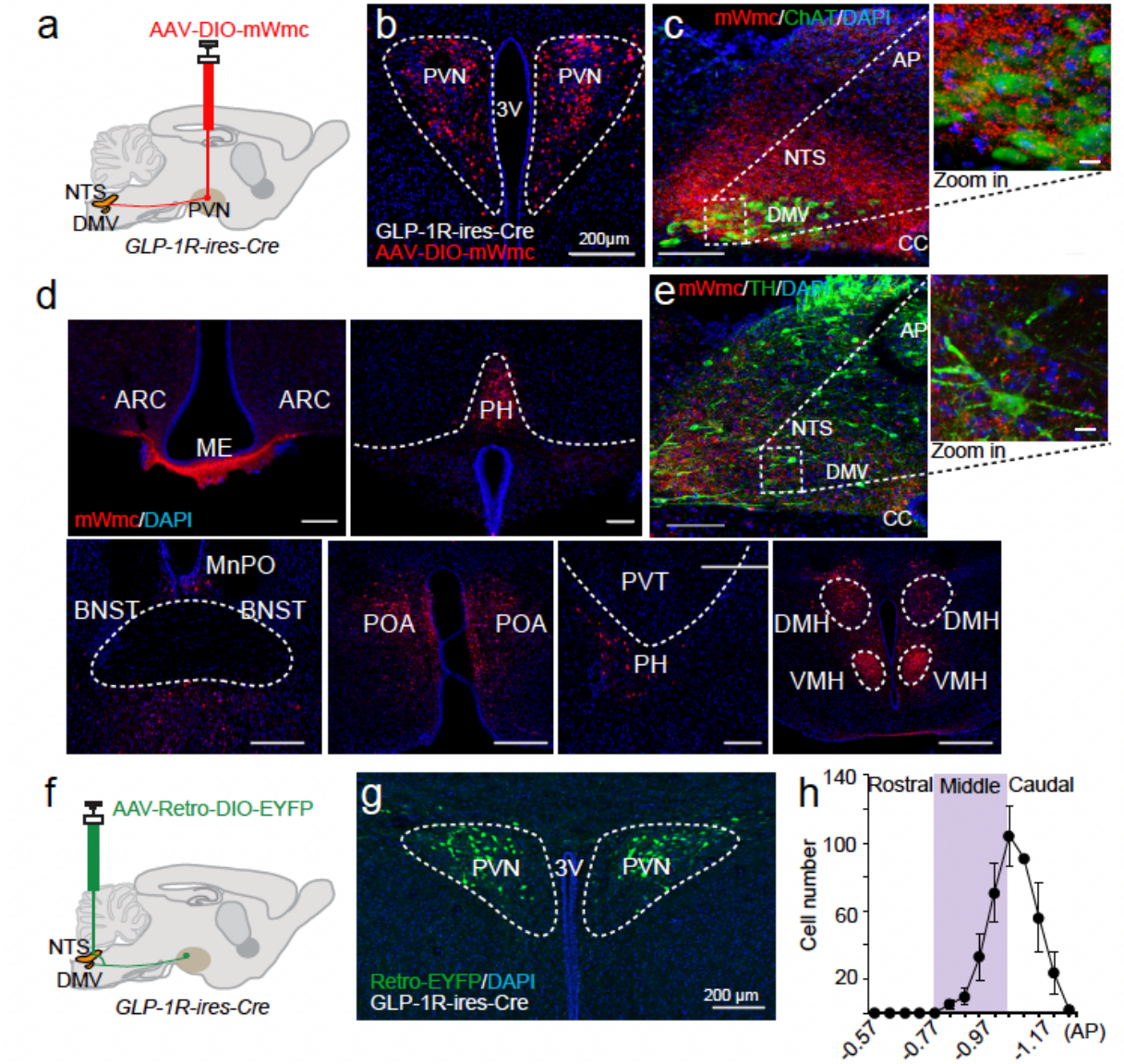

Extended Data Fig. 1: A survey of targets for PVN GLP-1R neuron projections. a. Experimental paradigm for anterograde trans-synaptic tracing. Trans synaptic AAV-DIO-mWGA-mCherry was injected into the PVN of GLP-1R-ires-Cre mice to map downstream neuronal targets. **b**. Representative image of the PVN section from the animal with AAV-DIO-mWGA-mCherry injections. **c-e**. Representative images of mWGA-mCherry labeling, downstream targets of PVN GLP-1R neurons, in the brain. **f**. Experimental paradigm for retrograde tracing of DVC inputs. AAV-Retro-DIO-EYFP was injected into the DVC in GLP-1-ires-Cre mice. **g**. Representative image of retrogradely labeled PVN GLP-R neurons that are projecting to the DVC. **h**. Quantification of anterior to posterior sections of $PVN^{GLP\text{-}1R}$→DVC neurons (n=3 mice). Data are presented as mean ± standard error of the mean (SEM).

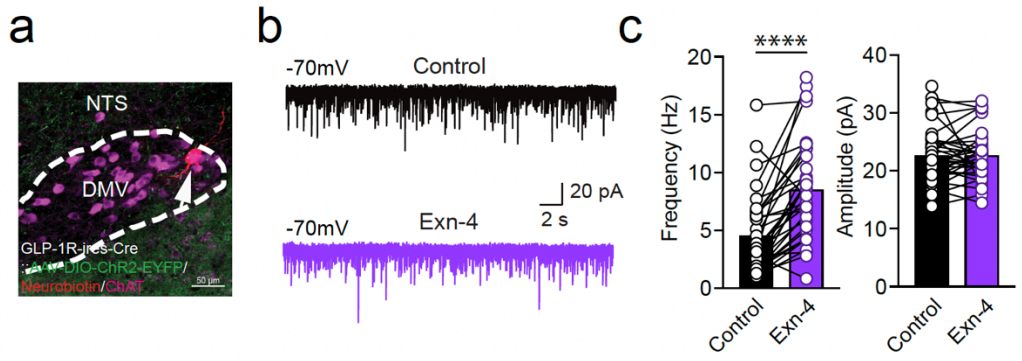

<u>Extended Data Fig. 2:</u> GLP-1R mediated signaling enhances DVC neuron synaptic inputs. **a**. Representative image of recorded DVC neurons labeled with neurobiotin. DMV neurons were visualized with ChAT immunostaining. **b**. Representative traces of sEPSCs with or without Exn-4 (100 nM). **c**. Pooled data of frequency and amplitude of sEPSCs recorded in DVC neurons. (n=34 cells/12 mice). Data are presented as mean ± standard error of the mean (SEM). Paired t-tests were used for statistics (**c**). ****p < 0.0001.

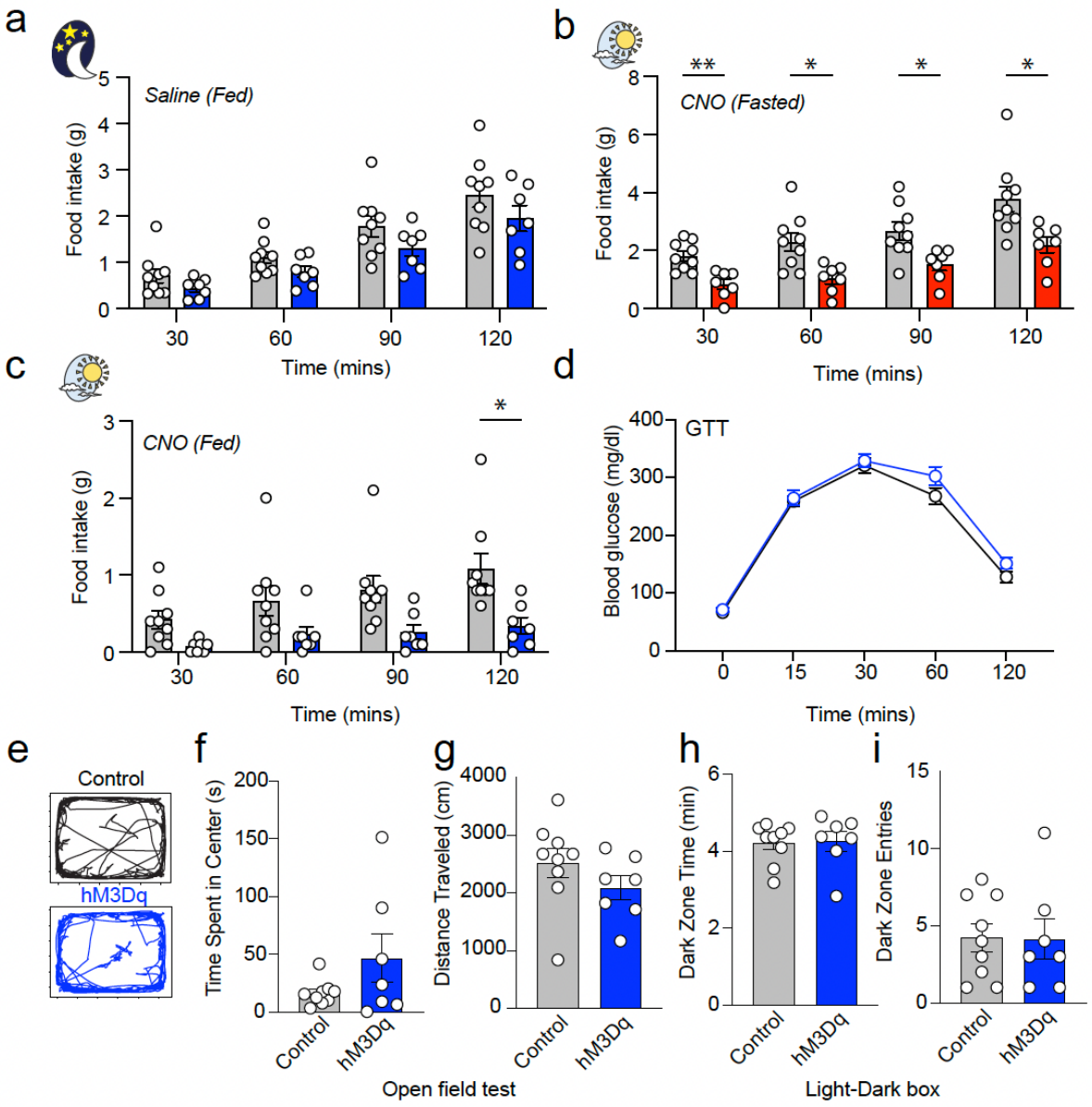

Extended Data Fig. 3: Chemogenetic activation of PVN$^{GLP\text{-}1R}$→DVC neurons via hM3Dq suppresses food intake. a-c. Food intake consumption upon activation of PVN$^{GLP\text{-}1R}$→DVC neurons under different energy states and times of the day with or without chemogenetic activation. **d**. Glucose tolerance test with or without chemogenetic activation. **e-g.** Representative traces of animal exploration in the open field with or without chemogenetic activation of PVN$^{GLP\text{-}1R}$→DVC neurons (e). Time spent in the center (f). Total traveled distance (g). **h&i**. Quantification of light-dark box assay for anxiety-like behaviors: time spent in dark zone (h) and dark zone entries (i). Data are presented as mean ± standard error of the mean (SEM). Control n=9 mice, hM3Dq n=7 mice.

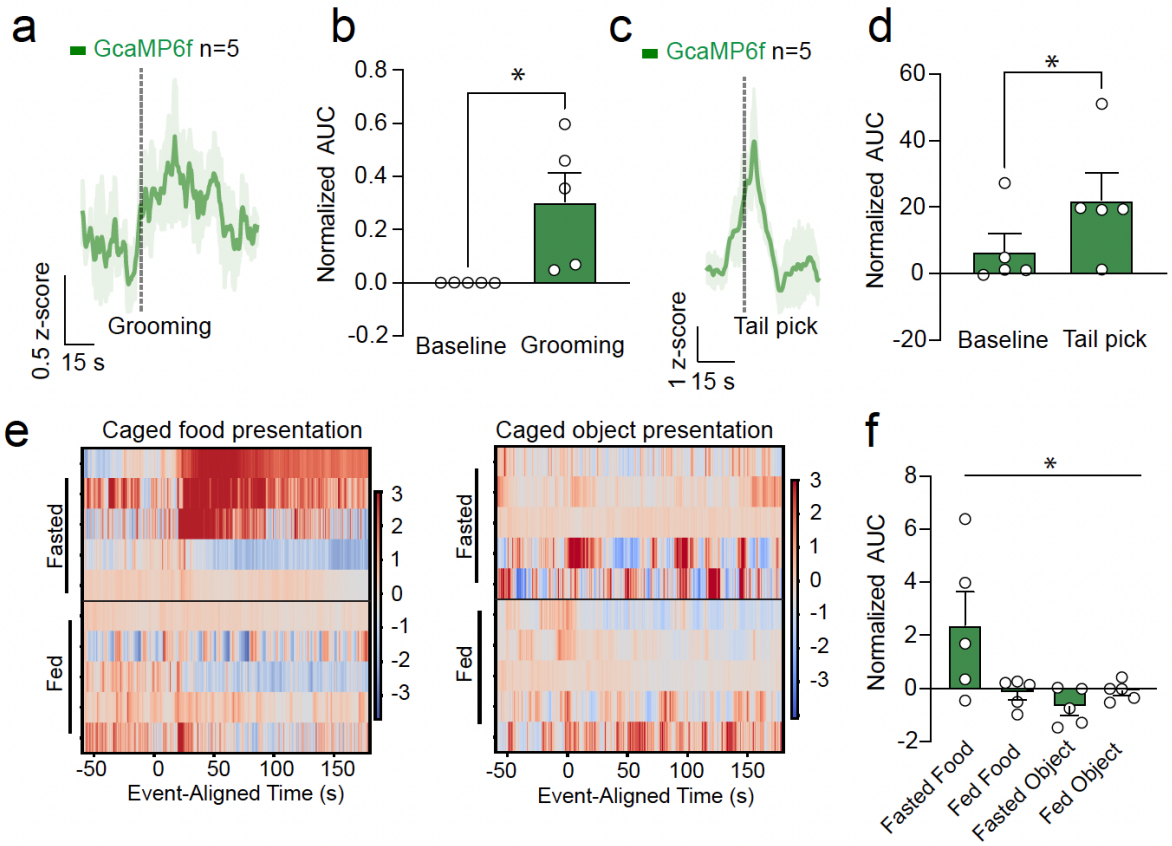

<u>Extended Data Fig. 4:</u> PVN$^{GLP\text{-}1R}$→DVC neurons respond to various sensory inputs. a-b. Fiber photometry data showing calcium dynamics of PVN$^{GLP\text{-}1R}$→DVC neurons during grooming behavior. **c-d**. Fiber photometry calcium dynamics of PVN$^{GLP\text{-}1R}$→DVC neurons during tail picking-induced stress. **e-f**. Calcium dynamics of PVN$^{GLP\text{-}1R}$→DVC neurons during different food/object tea ball drop stimuli across different energy states. Data are presented as mean ± standard error of the mean (SEM) and n=5 mice; Student's t-test (**b**, **d**); One-way ANOVA is applied to (**f**). *p< 0.05; **p<0.01.

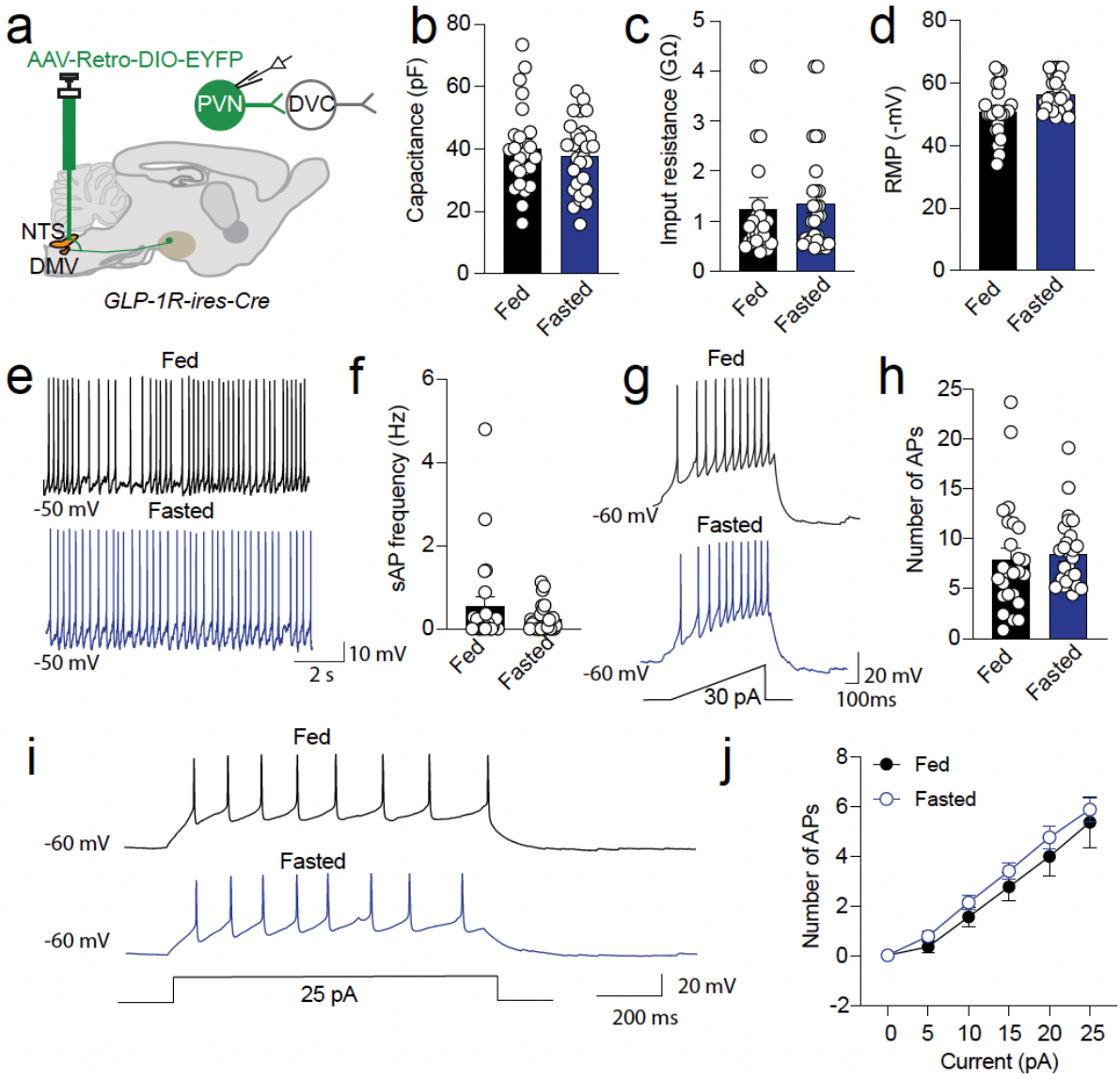

<u>Extended Data Fig. 5:</u> Electrophysiological characterization of PVN$^{GLP\text{-}1R}$→DVC neurons under different energy states. a. Experimental paradigm. **b-d**. Intrinsic electrophysiology characterization of PVN$^{GLP\text{-}1R}$→DVC neurons. Summary of capacitance (b) (Fed n=24 cells/3 mice, Fasted n=28 cells/3 mice), input resistance (c) (Fed n=24 cells/3 mice, Fasted n=28 cells/3 mice), resting membrane potential (d) (Fed n=24 cells/3 mice, Fasted n=28 cells/3 mice). **e.** Representative traces spontaneous action potentials (APs). **f**. Pooled data of sAP frequency (Fed n=24 cells/3 mice, Fasted n=28 cells/3 mice). **g.** Representative traces of neurons responding to ramping current injection. Insert show the current injection protocol. **h**. Quantification plot of ramping current injection action potential firing number (Fed n=25 cells/3 mice, Fasted n=27 cells/3 mice). **i,** Representative traces of neurons in response to stepped current injection. Insert show the current injection protocol. **j.** Pooled data of plot of the number of APs as a function of injected currents (Fed n=24 cells/3 mice, Fasted n=26 cells/3 mice). Data are presented as mean ± standard error of the mean (SEM).

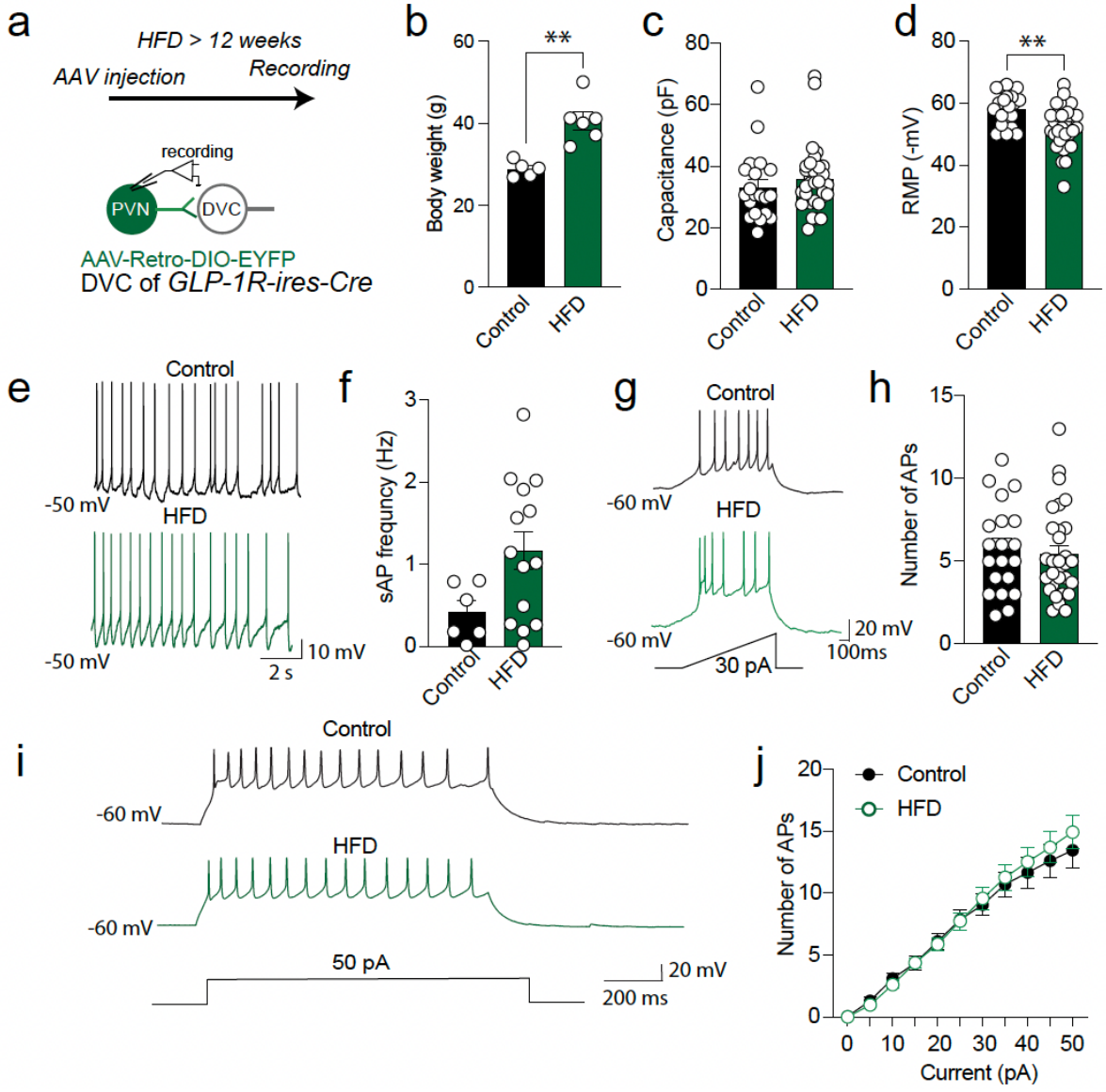

<u>Extended Data Fig. 6:</u> Electrophysiological characterization of PVN$^{GLP\text{-}1R}$→DVC neurons in HFD-induced obesity animals. a. Experimental paradigm. **b**. Body weight of control and HFD-induced obesity animals (Control n=5 mice, HFD n=5 mice). **c-d**. Intrinsic electrophysiology characterization of PVN$^{GLP\text{-}1R}$→DVC neurons. Summary of capacitance (c) (Control n=20 cells/3 mice, HFD n=32 cells/3 mice) and resting membrane potential (d) (Control n=20 cells/3 mice, HFD n=32 cells/3 mice) (Control n=20 cells/3 mice, HFD n=32 cells/3 mice). **e.** Representative traces spontaneous action potentials (APs). **f**. Pooled data of sAP frequency (Control n=6 cells/3 mice, HFD n=14 cells/3 mice). **g.** Representative traces of neurons respond to ramp current injection. Insert show the current injection protocol. **h**. Quantification plot of ramp current injection action potential firing number (Control n=20 cells/3 mice, HFD n=30 cells/3 mice). **i,** Representative traces of neurons in response to step current injection. Insert show the current injection protocol. **j**. Pooled data of plot of the number of APs as a function of injected currents (Control n=20 cells/3 mice, HFD n=30 cells/3 mice). Data are presented as mean ± SEM and sample sizes are indicated in each plot.

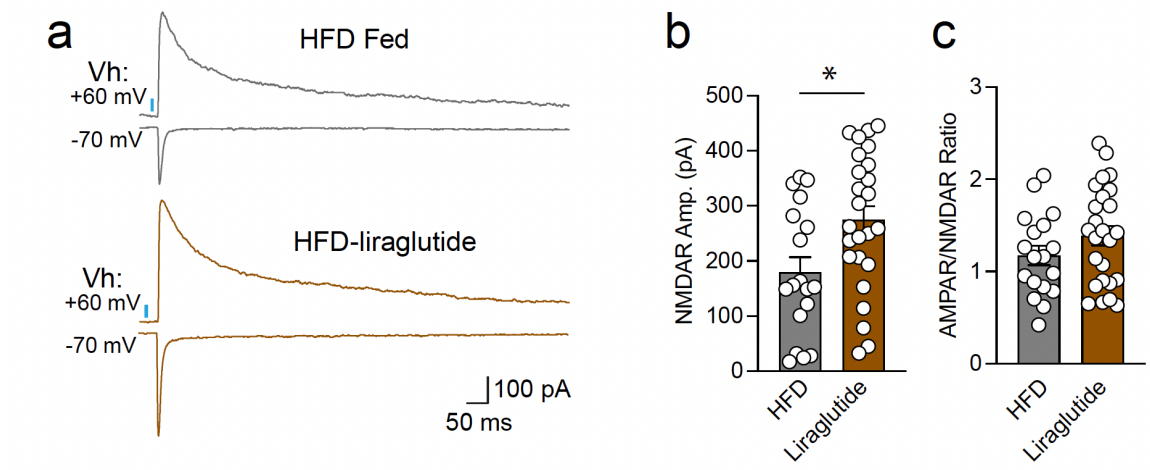

Extended Data Fig. 7: Liraglutide augments PVN$^{GLP\text{-}1R}$→DVC synaptic release in HFD-induced obese animals. a. Representative traces of AMPAR-oEPSCs and NMDAR oEPSCs in HFD-fed induced obese animals with or without Liraglutide (i.p. 400 ug/kg) administering. after i.p. injection of 400 ug/kg liraglutide. **b-c**. Pooled data of NMDAR-oEPSCs (HFD n=18 cells/3 mice, Liraglutide n=25 cells/3 mice). and AMPAR/NMDAR oEPSCs ratio (HFD n=18 cells/3 mice, Liraglutide n=18 cells/3 mice). Data are presented as mean ± SEM. Student's t-test (**b-c**). *p< 0.05.

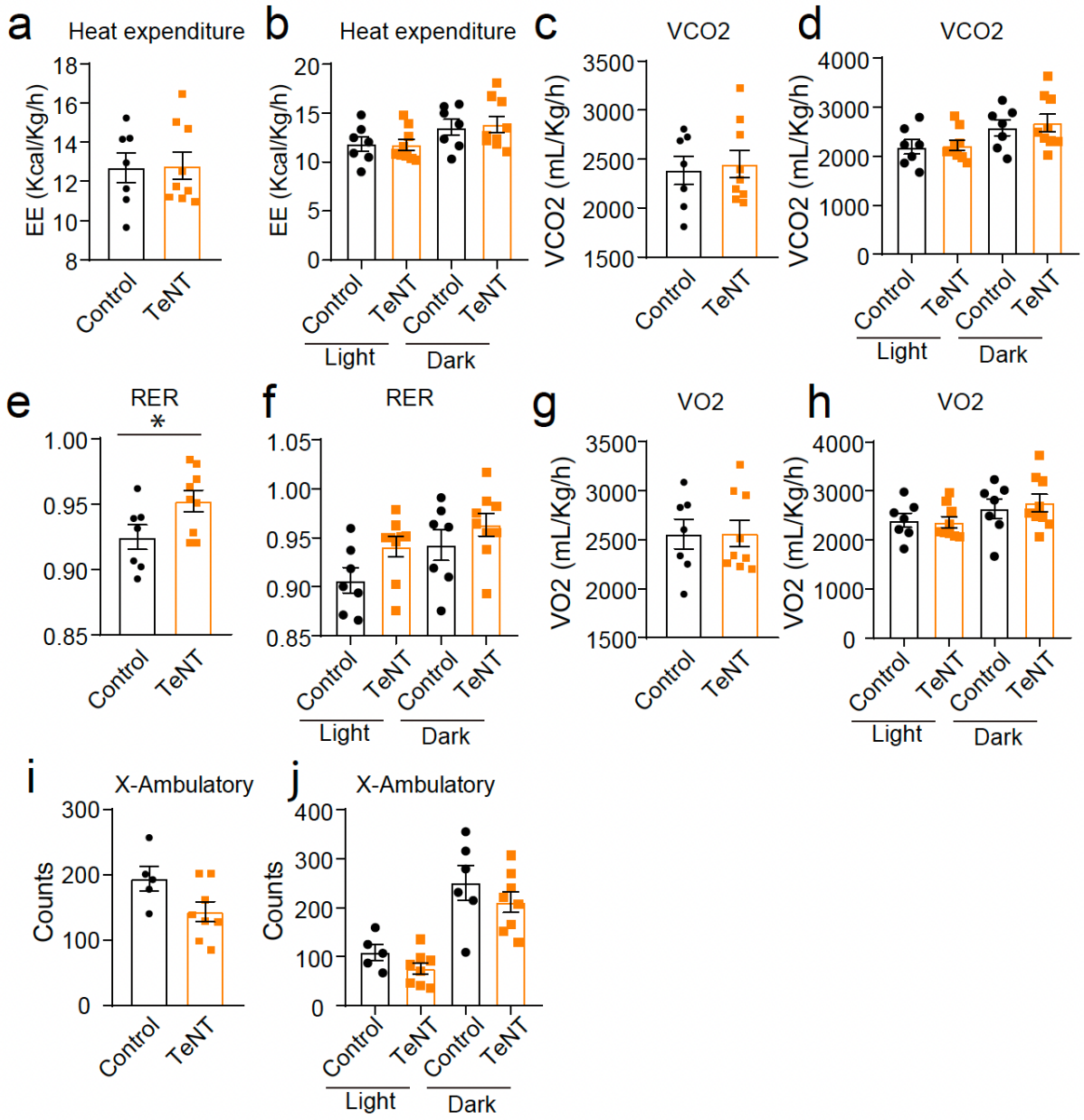

Extended Data Fig. 8: Comprehensive metabolic analyses of animals after inactivation of PVN$^{GLP\text{-}1R}$→DVC synaptic release using Comprehensive Lab Animal Monitoring System (CLAMS). a-b. Average energy expenditure (EE). **c-d**. The volume of carbon dioxide produced (VCO2). **e-f**. Respiratory exchange ratio (RER). **g-h**. Oxygen consumed (VO2). **i-j**. Average locomotor activity of TeNT and control (GFP) animal. Control n=7 mice, TeNT n=9 mice. Data are presented as mean ± SEM and sample sizes are indicated in each plot; Student's t-test is applied to (**e**). *p< 0.05.